Group 4 Metal Complexes Bearing Thioetherphenolate Ligands. Coordination Chemistry and Ring-Opening Polymerization Catalysis

ARTICLE *in* MACROMOLECULES · APRIL 2014

Impact Factor: 5.8 · DOI: 10.1021/ma5003358

Macromolecules

Article

pubs.acs.org/Macromolecules

Group 4 Metal Complexes Bearing Thioetherphenolate Ligands. Coordination Chemistry and Ring-Opening Polymerization Catalysis

Francesco Della Monica,[†] Ermanno Luciano,[†] Giuseppina Roviello,[‡] Alfonso Grassi,[†] Stefano Milione,*[,†] and Carmine Capacchione[†]

[†]Department of Chemistry and Biology, University of Salerno, via Giovanni Paolo II, 132 Fisciano I-84084, Salerno, Italy

[‡]Department of Engeneering, University of Naples, Parthenope Centro Direzionale Napoli Isola C4, 80143 Napoli, Italy

Supporting Information

ABSTRACT: A series of group 4 metal complexes **1**−**4** (**1** = $(^{t\text{-Bu}}OS)_2Ti(O\text{-}i\text{-}Pr)_2$; **2** = $(^{t\text{-Bu}}OS)_2Zr(O\text{-}t\text{-}Bu)_2$; **3** = $(^{t\text{-Bu}}OS)_2Hf(O\text{-}t\text{-}Bu)_2$; **4** = $(^{Cum}OS)_2Zr(O\text{-}t\text{-}Bu)_2$) supported by two phenolate bidentate ligands ($^{t\text{-Bu}}OS$−H = 4,6-di-*tert*-butyl-2-phenylsulfanylphenol and ^{Cum}OS−H = 4,6-dicumyl-2-phenylsulfanylphenol) were synthesized by the reaction of appropriate metal tetra(alkoxide)s with 2 equiv of the ligands. The X-ray structure of **2** revealed that the two ligands were κ^2-chelated to the metal center with two phenoxy groups in trans positions and the two thioether moieties in cis positions. VT NMR analysis revealed a fast inversion of configuration at the metal center. Complexes **1**−**4** promoted the ring-opening polymerization (ROP) of lactide and ε-caprolactone. Complex **4** exhibited the highest activity with a pseudo-first-order rate constant of 0.061 ± 0.003 min^{-1} at 100 °C, which compares favorably with those reported for the most active group 4 complexes. Polymerizations were well-controlled, giving predictable molecular weights and narrow molecular weight distributions. Essentially atactic PLA were obtained in the ROP of *rac*-lactide. A DFT study on ROP promoted by these complexes highlighted the importance of the coordinative flexibility of the ancillary ligand to promote monomer coordination at the reactive metal center. In presence of isopropanol, lower PDI indexes and molecular weights of the PLAs proportional to the equivalents of isopropanol suggested that adequate conditions for effective "*immortal*" polymerizations were achieved. More interestingly, these catalysts promoted the copolymerization of L-lactide and ε-caprolactone. The microstructure disclosed by ^{13}C NMR analysis and the thermal behavior exhibited in DSC studies indicated a random distribution of the two monomer along the polymer chain.

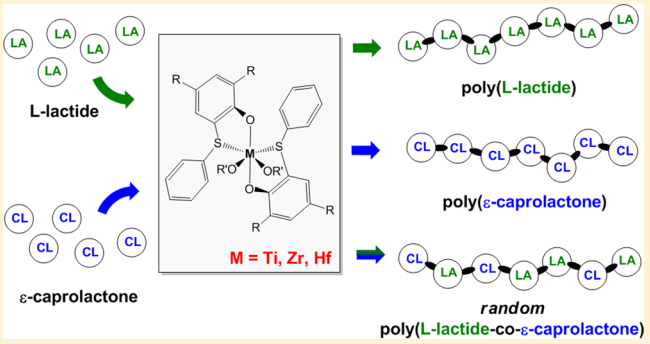

INTRODUCTION

Plastics are essential in the everyday life being employed in many domestic and industrial applications. Nowadays, their production is still dominated by polyolefins whose derivation from nonrenewable sources and after-use disposal raise several economic and environmental concerns.[1] Sustainability of raw materials and environmental impact of discarded plastic waste in landfills have driven the academic research toward the development of new materials with comparable performance, if not superior, to those of conventional oil-based polymers.[2] The aliphatic polyesters, such as polylactide (PLA), polycaprolactone (PCL), and their copolymers, are among the most promising polymers in this field. Thanks to their good mechanical properties, biodegradability, and biocompatibility, PCL and PLA have found wide applications as commodity polymers for short-time applications (e.g., packaging, fibers) and as engineering materials in biomedical and pharmaceutical fields for the production of resorbable surgical sutures, controlled drug release systems, and scaffolds for tissue engineering.[3] Although polyesters can be produced by condensation polymerization or ring-opening polymerization (ROP) of the related cyclic esters using anionic, cationic, and organic compounds as initiators, the most efficient method to synthesize aliphatic polyesters with controlled properties is the ROP promoted by metal complexes.[4] Among the large variety of metal complexes investigated as initiators, group 4 metal complexes have been shown to be particularly attractive thanks to their low toxicity and good control over polymerization process.[5] Despite these metals being recognized to give potentially active complexes, only a limited number of studies have examined their performances in the ROP of cyclic esters. Typically, catalysts are composed of phenoxo-type chelating ligands and labile alkoxo groups. Because of the hard Lewis acidic nature of the group 4 metal, phenoxo donors tend to be matched with relatively hard first-row nitrogen-based donors.[5] Recent studies have evidenced that the introduction of soft second-row donors in the coordination sphere of oxophilic metal center may be beneficial for the catalytic activity as they

Received: February 13, 2014
Revised: April 7, 2014
Published: April 16, 2014

   dx.doi.org/10.1021/ma5003358 | *Macromolecules* 2014, 47, 2830−2841

could mediate the Lewis acidity of the metal center with intriguing influence on the catalytic reactivity.[6] Results by Kol et al. showed that the complexation of group 4 metals to tetradentate dithiodiolate ligands gave extremely active initiators for lactide polymerization with full consumption of 300 equiv of monomers in the melt after 17 min for the Ti complex and 1 min for the Hf derivative.[7] Okuda et al. reported that titanium and zirconium complexes bearing tetradentate (OSSO)-type bis(phenolato) ligands efficiently initiate the ring-opening polymerization of lactide monomers in a controlled fashion.[8] Syndiotactic poly(*meso*-LA) was produced in polymerization of *meso*-lactide by OSSO−titanium complexes whereas heterotactically biased PLA was produced when the polymerization was initiated by OSSO−zirconium complexes.[8] The catalytic activity was strongly dependent on the ligand backbone. Systematic variation of the bridge between the two phenolate groups indicated that a more flexible ligand skeleton renders the catalyst more active (1,2-cyclohexanediyl < 1,2-ethanediyl < 1,3-propanediyl).[8]

In this contest, monoanionic OS-bidentate ligands appear as potential candidates for coordination to oxophilic group 4 metals for the possible use of the derived complexes in catalysis. Herein we show that the absence of the bridging link between the two phenoxo units produces flexible and labile coordination geometry around the metal center with remarkable consequences on the catalytic performances. In this paper, we describe the synthesis and structural characterization of a series of group 4 metal complexes supported by *o*-thioetherphenolate ligand and their use in the ROP of cyclic esters. The coordination chemistry was explored in the solid state by X-ray diffraction studies and in solution by variable-temperature NMR analysis. Finally, we demonstrate the utility of the title initiators for the copolymerization of L-lactide with *ε*-caprolactone. To the best of our knowledge, this is the first example of zirconium complex able to produce random copolymers from L-lactide and *ε*-caprolactone.

RESULTS AND DISCUSSION

Syntheses and Characterization. Two *o*-thiophenol ligands, $^{t\text{-Bu}}$OS-H = 4,6-di-*tert*-butyl-2-phenylsulfanylphenol and ^{Cum}OS-H = 4,6-dicumyl-2-phenylsulfanyphenol, were prepared by reacting the appropriate lithium phenoxide with benzenesulfenyl chloride.[9]

Alkoxide derivatives of the group 4 metal complexes are generally prepared by alcoholysis of homoleptic tetraalcoholates $M(OR)_4$.[10] ^{1}H NMR monitoring of the reaction between $^{t\text{-Bu}}$OS-H ligand and Zr(O-*t*-Bu)$_4$ showed that it is fast and quantitative in few minutes and that the formation of the octahedral diligand chelated complex is favorite regardless of the $^{t\text{-Bu}}$OS-H/Zr(O-*t*-Bu)$_4$ molar ratio. The reaction of $^{t\text{-Bu}}$OS-H with Zr(O-*t*-Bu)$_4$ in 2:1 molar ratio gave ($^{t\text{-Bu}}$OS)$_2$Zr(O-*t*-Bu)$_2$ as the only reaction product while the 1:1 molar ratio afforded a mixture of mono- and disubstituted complexes in a 1:2 molar ratio. When Zr(O-*t*-Bu)$_4$ was treated with 3 equiv of $^{t\text{-Bu}}$OS-H ligand, a mixture of disubstituted complex and unreacted ligand was obtained. The ^{1}H−^{1}H EXSY experiment of this reaction mixture (C_6D_6, τ_m = 0.65 s) revealed the existence of exchange regime between *tert*-butanol and ($^{t\text{-Bu}}$OS)$_2$Zr(O-*t*-Bu)$_2$. As shown in Figure 1, a positive cross-peak clearly correlates the signals of *tert*-butanol and of the *tert*-butoxy group bound to the zirconium atom. The intensity of this peak permitted to calculate the rate constant for the ligand exhange reaction. The values of 0.33 s^{-1} was obtained. The lack of cross-peaks between the free and coordinated ligands ruled out this exchange process.

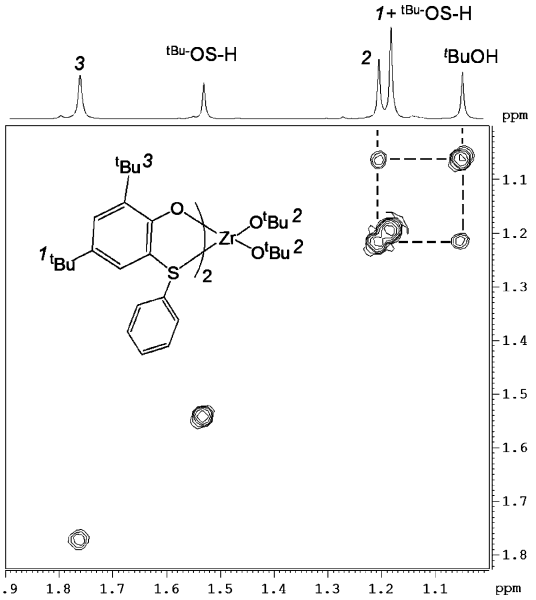

Figure 1. ^{1}H−^{1}H EXSY spectrum of ($^{t\text{-Bu}}$OS)$_2$Zr(O-*t*-Bu)$_2$, $^{t\text{-Bu}}$OS-H, and *t*-BuOH mixture (1:1:2, C_6D_6, rt, mixing time = 0.65 s, 400 MHz). The exchange of the *t*-BuO group for ($^{t\text{-Bu}}$OS)$_2$Zr(O-*t*-Bu)$_2$/$^{t\text{-Bu}}$OS-H is evidenced ($k_{exchange}$ = 0.33 s^{-1}).

The titanium, zirconium, and hafnium complexes **1**−**4** (**1** = ($^{t\text{-Bu}}$OS)$_2$Ti(O-*i*-Pr)$_2$; **2** = ($^{t\text{-Bu}}$OS)$_2$Zr(O-*t*-Bu)$_2$; **3** = ($^{t\text{-Bu}}$OS)$_2$Hf(O-*t*-Bu)$_2$; **4** = (^{Cum}OS)$_2$Zr(O-*t*-Bu)$_2$) were synthesized by treatment of the ligands with Ti(O-*i*-Pr)$_4$, Zr(O-*t*-Bu)$_4$, or Hf(O-*t*-Bu)$_4$ in good yield (see Scheme 1). Zr(O-*t*-Bu)$_4$ and Hf(O-*t*-Bu)$_4$ were chosen as starting reagents to avoid the use of ill-defined Zr(O-*i*-Pr)$_4$ and Hf(O-*i*-Pr)$_4$ species. The complexes **1**−**4** were isolated as white solids and purified by pentane washings followed by drying in high vacuum to remove residual M(OR)$_4$ and alcohols which could affect the activities in the polymerization tests.

Scheme 1

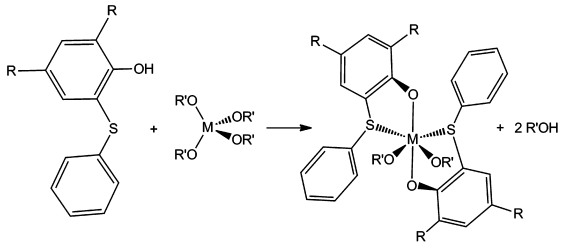

M = Ti, R' = *i*-Pr, R = *t*-Bu (**1**)
M = Zr, R' = *t*-Bu, R = *t*-Bu (**2**)
M = Hf, R' = *t*-Bu, R = *t*-Bu (**3**)
M = Zr, R' = *t*-Bu, R = CMe_2Ph (**4**)

Single crystals of **2** were grown from a saturated pentane solution at −20 °C. The molecular structure of the complex **2** is reported in Figure 2. The complex crystallizes in a monoclinic system (space group *C*2/*c*). The asymmetric unit contains a half molecule of the zirconium complex and a disordered half pentane molecule, both lying on an a crystallographic glide plane. The coordination environment of the zirconium atom is

dx.doi.org/10.1021/ma5003358 | Macromolecules 2014, 47, 2830−2841

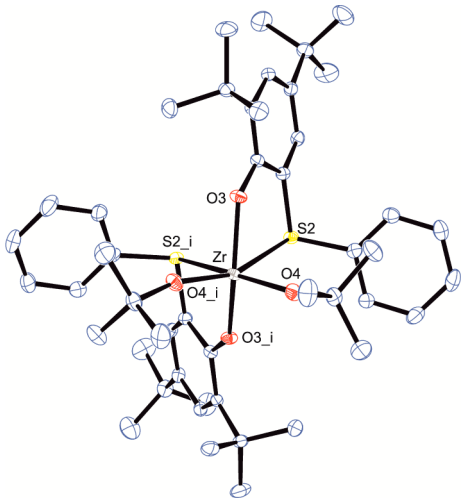

Figure 2. ORTEP-3 view of **2**. Thermal ellipsoids are shown at 30% probability level. Hydrogen atoms and a pentane crystallization molecule lying on a glide plane are omitted for clarity. Symmetry transformation used to generate equivalent atoms: _i: $-x, y, -z + 1/2$. Selected bond distances and angles (Å, deg): Zr–O4 = 1.904(2); Zr–O3 = 2.022(2); Zr–S2 = 2.965(1); O3–Zr–O4_*i* = 98.7(1); O3–Zr–S2 = 68.6(5); S2–Zr–O3_*i* = 83.5(1); O3–Zr–O4 = 100.9(1); O4–Zr–S2_*i* = 157.1(1); O3–Zr–O3_*i* = 147.1(1).

strongly distorted octahedral due to steric hindrance of the OS bidentate ligands. The complex shows a C_2-symmetrical configuration with two *cis* arranged *t*-BuO groups (O4–Zr1–O4_*i* = 105.85°). In agreement with the electron-withdrawing properties of the aryl group bound to the sulfur atoms, the Zr–S distances, both of 2.965 Å, are slightly longer than those observed in the corresponding complex in which the two sulfur atoms are linked by an ethyl bridge ({S-Et-S}(4,6-^{t}Bu$_2$-PhO)$_2$Zr(O^{t}Bu)$_2$, Zr1–S1 2.877(1) Å and Zr1–S2 2.837(1) Å).[8a] The other bond distances and angles are similar to those reported in the literature for analogous complexes.[8a]

Solution Structures. Six-coordinate bis(chelate) complexes can have up to five distinct configurational isomers differing in the geometrical disposition of the ligands. In two of these isomers the two monodentate ligands are located *trans* to one another on the octahedron, in the other three cases the monodentate ligands are *cis* to one another. The isomers displaying the *cis* arrangement are chiral. Frequently these complexes have stereochemically nonrigid coordination environment at the metal center; in solution, they can present different isomers or display fluxional process.[11] For these reasons we investigated the solution structure of complexes **1**–**4**.

In the ^{1}H NMR spectra of complexes **1**–**3** the resonances due to the phenoxy–thioether ligands were unequivocally recognized and found significantly shifted with respect to the signals of the protons of free ligands. In particular, the *ortho* protons of the S–C$_6$H$_5$ group were downfield shifted, indicating the coordination of the sulfur donor of the chelating ligand to the metal center. In the ^{1}H NMR spectrum of complex **1**, the isopropoxy groups produce a heptet and a doublet centered at 4.58 and 1.17 ppm, respectively, whereas the *tert*-butoxy in **2** and **3** appeared as singlet at 1.22 ppm. Cooling solutions of **1**–**3** in CD_2Cl_2 to −80 °C did not produce new ^{1}H NMR patterns, indicating the presence of a unique isomer further confirmed by the observation of a single set of resonances in the ^{13}C NMR spectra. When the solution **1** was cooled at subambient temperature, the ^{1}H methyl signal of isopropoxy groups broadened and resolved in two doublets (see Supporting Information); the coalescence of these signals was observed at −70 °C. This indicates that complex **1** adopts the same coordination geometry (trans-O,O, cis-S,S, cis-O^{iPr},O^{iPr}) observed in the solid state for **2** and that a fast inversion of configuration at the metal center is operative at room temperature likely via a tetrahedral transition state. A similar behavior was observed for tetradentate [OSSO] titanium complexes with a 5–6–5 or 6–5–6 array of chelate rings that were fluxional at room temperature.[12,13]

The ^{1}H NMR spectrum of complex **4** features broad resonances at room temperature probably due to the stereorigid environment at the metal center determined by the sterically hindred cumyl groups. It is reasonable to assume that the fluxional process observed for **1** is active for all complexes.

Ring-Opening Polymerization of Lactide. The performances of **1**–**4** in the ROP of L-lactide were investigated under a standard set of conditions: 0.52 M LA lactide in toluene solution using an initiator concentration of 5.2 mM. Representative results are reported in Table 1. The polymerization runs were tracked by analyzing the product mixtures sampled from the reactor at certain reaction times. Each aliquot was quenched with wet $CDCl_3$ and analyzed by ^{1}H NMR spectroscopy to determine the LA conversion. Moreover, the GPC analysis of the polymer products allowed to determine the number-average molecular weight ($M_{n(expt)}$) and the polydispersity index (PDI = M_w/M_n) values. The titanium complex **1** initiated the ROP of LA converting 100 equiv of monomer in 8 h at 100 °C (Table 1, run 1). In Figure 3 the semilogarithmic plot of $\ln([\text{L-LA}]_0/[\text{L-LA}]_t)$ versus time was linear, showing a pseudo-first-order kinetics in LA with a k_{obs} of $(3.96 \pm 0.05) \times 10^{-3}$ min^{-1}. The experimental number-average molecular weights ($M_{n(expt)}$) increased linearly with monomer conversion (see Figure S7 in Supporting Information) and were in good agreement with the theoretical values ($M_{n(calc)}$) calculated assuming two polymer chains per Ti initiator. The PDIs were low, indicative of well-controlled polymerization. End-group analyses of PLA by ^{1}H NMR spectroscopy revealed the presence of the isopropyl ester end group (δ 5.08 for methine and δ 1.24 for methyl), proving that the initiation step involves the insertion of the coordinated monomer into the Ti–O^{i}Pr bond. The catalytic performance of complex **1** well compares, in terms of activity and control over polymerization process,

Table 1. Ring-Opening Polymerization of L-Lactide by 1–4

entry[a]	initiator	T/°C	t/h	conv/%[b]	$M_{n,th}$[c]	$M_{n,GPC}$[d]	PDI[d]
1	**1**	100	8.0	84	6.1[e]	6.0	1.18
2	**2**	100	1.25	90	13.0	8.9	1.10
3	**2**	80	3.0	89	12.8	15.3	1.44
4	**2**	25	120	73	10.5	10.2	1.43
5	**3**	100	1.5	82	11.7	8.1	1.24
6	**4**	100	0.5	86	12.4	10.8	1.18

[a]All reactions were carried out in 2.4 mL of toluene, $[I]_0$ = 5.2 mM, [LA] = 0.52 M, $[LA]/[I]_0$ = 100. [b]Molecular conversion determined by ^{1}H NMR spectroscopy ($CDCl_3$, 298 K). [c]Calculated molecular weight using $M_{n,th}$ (kg mol^{-1}) = 144.13 × $([LA]_0/[I]_0)$ × LA conversion. [d]Experimental molecular weight M_n and polydispersity (PDI) determined by GPC in THF using polystyrene standards and corrected using a factor of 0.58. [e]$M_{n,th}$ (kg mol^{-1}) = 144.13 × $([LA]_0/[2 \times I]_0)$ × LA conversion.

dx.doi.org/10.1021/ma5003358 | *Macromolecules* 2014, 47, 2830–2841

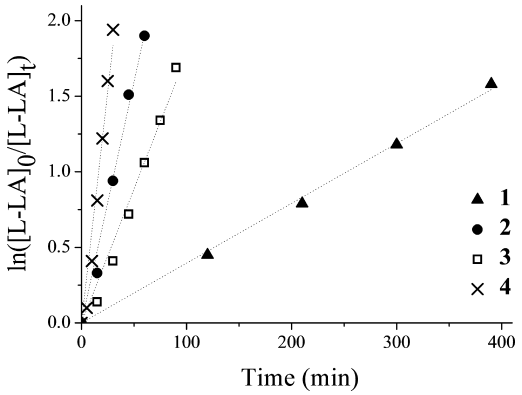

Figure 3. Pseudo-first-order kinetic plots for ROP of LA promoted by complexes **1**–**4**. The pseudo-first-order rate constants are k_{obs}(**1**) = (3.96 ± 0.05) × 10^{-3} min^{-1} (R = 0.999), k_{obs}(**2**) = 0.032 ± 0.001 min^{-1} (R = 0.995), k_{obs}(**3**) = 0.0177 ± 0.0006 min^{-1} (R = 0.992), and k_{obs}(**4**) = 0.061 ± 0.003 min^{-1} (R = 0.985). Conditions: $[I]_0$ = 5.2 mM; $[LA]_0/[I]_0$ = 100; toluene as solvent; T = 100 °C.

with those of other Ti–alkoxide complexes in the ROP of lactide.[5,14]

As expected, the zirconium complex **2** was much more active than **1** and showed high monomer conversion in 1 h. This finding is in line with the head to head comparison of similar Ti and Zr complexes[5] and is attributed to the most facile access of the monomer to the bigger metal center. It is worth noting that the analogous [OSSO]–zirconium complexes resulted moderately active requiring several hours at high temperature to reach high conversions.[8] The monomer consumption followed a first-order kinetics, with instantaneous initiation (k_{obs} = 0.032 ± 0.001 min^{-1}); moreover, the plot of $M_{n(expt)}$ vs percent conversion was linear. PDIs were narrow throughout the course of the polymerizations, with value in the range 1.10–1.16. The $M_{n(expt)}$ were slightly lower than expected for one chain growing for metal center, suggesting a partial triggering of the second active site on the metal center (see Figure S8 in Supporting Information). By lowering the polymerization temperature at 80 °C, a decreases in catalytic activity was observed (see Figure S9 in Supporting Information). The propagation rate constant decreased to 0.012 ± 0.001 min^{-1}, and a short induction period of about 20 min was observed. The $M_{n(expt)}$ linearly increased with conversion but were systematically higher than predicted. This deviation and the presence of an induction time suggest a poor initiation rate compared to propagation. At 25 °C, the rate constant was (1.75 ± 0.04) × 10^{-4} min^{-1}. The catalyst showed no sign of decomposition and resulted active for days. High monomer conversions were reached after 5 days: under these conditions an excellent agreement between the experimental and the theoretical masses was achieved. The overall results proved that a controlled polymerization mechanism was obtained.

The nature of initiating group was investigated by ESI-mass spectrometry of oligomers by **2** at 100 °C with $[L\text{-}LA]_0/[I]_0$ = 10. A narrow but asymmetric monomodal distribution of Na^+ adducts was detected in the range 500–1500 Da with a regular mass-to-mass peak increment of 72 Da (see Figure S10 in Supporting Information). The peaks were consistent with the presence of linear both even-membered and odd-membered oligomers terminated by hydroxy and *tert*-butoxide as chain end groups, i.e., H–[OCH(CH_3)C(=O)]$_n$–O^{t}Bu. This suggests that (i) the polymerization is initiated by the transfer of an alkoxide group to the monomer and follows a coordination–insertion mechanism and (ii) inter- and intramolecular transesterification side reactions take place during the propagation processes.

To further investigate the catalytic performances of **2**, the influence of monomer-to-initiator ratio on the polymerization was explored. The $M_{n(expt)}$ of the resulting PLA increased linearly with the $[M]_0/[I]_0$ ratio ranging from 100 to 750, while the molecular weight distributions remained almost unchanged (see Figure S11 in Supporting Information). At high $[M]_0/[I]_0$ ratio the molecular weights were lower than those calculated, indicating a loss of control probably due to the activation of the second active site on the metal center.

Switching from zirconium to hafnium, the polymerization rate in ROP of LA marginally decreased (Figure 3): the complex **3** allowed 82% monomer conversion in 1.5 h at 100 °C. All experimental data support a well-controlled L-LA ROP process. The kinetics was first-order in LA with a pseudo-first-order rate constant of 0.0177 ± 0.0006 min^{-1}. The resulting polymers showed monomodal and quite narrow molecular weight distributions (M_w/M_n = 1.17–1.24) with molecular weights that correlated with those calculated on the basis of the initial monomer-to-initiator ratio and conversion (see Figure S12). Also in this case, at high conversions the molecular weight deviated from those calculated, suggesting a partial activation of the second active site on the metal center.

On inspection of Figure 3 and Table 1, the replacement of ^{t}Bu groups by cumyl groups resulted in a beneficial effect in terms of catalytic activity; in fact, complex **4** catalyzed the polymerization of L-lactide significantly faster than complexes **2** and **3** with a pseudo-first-order rate constant of 0.061 ± 0.003 min^{-1} at 100 °C. Complex **4** compares well with the most active group 4 complexes reported so far for the polymerization of lactide.[7,15]

The $M_{n(expt)}$ showed a better agreement with the theoretical values than those observed for complex **2** (Figure 4). It is

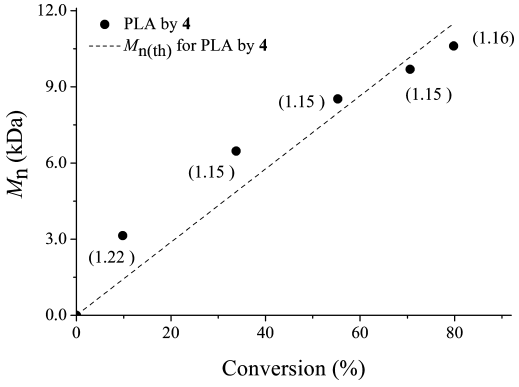

Figure 4. Plot of number-averaged molecular weights M_n vs monomer conversion using **4** for L-LA polymerization. M_w/M_n values are in parentheses. Conditions: $[I]_0$ = 5.2 mM; $[LA]_0/[I]_0$ = 100; toluene as solvent; T = 100 °C.

reasonable to hypothesize that the introduction of bulkier *o*-substituent on the phenoxy moiety prevents effectively the inter/intramolecular transesterification side reactions and therefore benefits the coordination/insertion of monomer.[16] This result together with a linear correlation between the molecular weight number of the polymer chain, the monomer-to-polymer conversion, reasonably narrow polydispersity, and a

dx.doi.org/10.1021/ma5003358 | Macromolecules 2014, 47, 2830–2841

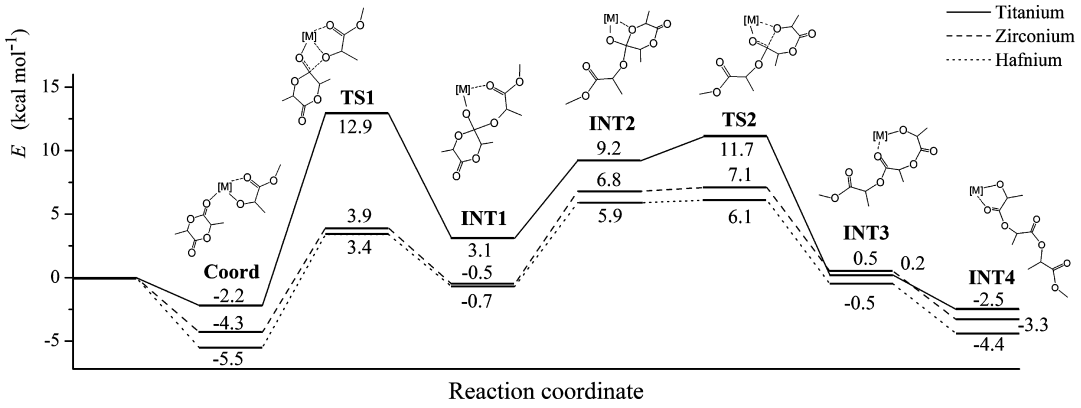

Figure 5. Energy profiles of L-lactide ring-opening polymerization.

first-order dependence on monomer concentration support a well-controlled polymerization process.

Polymerization of *rac*-lactide (*rac*-LA) was also explored to assess stereocontrol of the polymerization. As with L-lactide, the complexes **1**−**4** catalyze the ROP of *rac*-LA in controlled manner, as assessed by well behaved first-order kinetics, linear M_n vs time plots, and relatively narrow PDIs in the range ca. 1.1−1.2. Disappointingly, the PLAs by **1**−**3** were atactic ($P_r \approx 0.50-0.55$). The more sterically encumbered complex **4** afforded a heterotactic biased polymer with $P_r = 0.62$. The influence of ligand framework on the stereoselectivity was less pronounced than that exerted on the activity.

DFT Calculations: Energy Profiles of the Lactide Ring-Opening Polymerization. In order to gain further insight into the role played by the thioetherphenolate ligand, a DFT investigation of the ROP of lactide promoted by this class of complexes was carried out. The monomer coordination is a prerequisite necessary for the ring-opening step. We succeeded in locating the coordination adducts only when one of the two ligands was considered to be η^1-coordinated to the metal atom. In these species the metal center is in an octahedral coordination environment with the monomer and the growing chain located in *cis* positions (Ti···O_{LA} = 2.384 Å, Zr···O_{LA} = 2.391 Å, Hf···O_{LA} = 2.330 Å). Compared to the starting reagents, the monomer coordination was predict to be exothermic (−2.2 (Ti); −4.3 (Zr); −5.5 (Hf) kcal mol^{-1}). These structures were used as starting points for the DFT calculations. The intermediates and transition states found for the ring-opening process were similar to those reported in the literature.[17] The energy profiles are displayed in Figure 5, and the transition states for the model zirconium complex are shown in Figure 6. The propagation step started with the nucleophilic attack of the lactate unit at the activated carbonyl carbon of the coordinated L-LA. At the transition state, the C═O_e bond was slightly elongated, reflecting the rehybridization of C═O from sp^2 toward sp^3 (Figure 6). Transition state **TS1** was the highest point of the reaction profile in all cases. Coherently with the experimental results, the activation barrier found for the titanium complex (15.1 kcal mol^{-1}) was higher than the corresponding ones obtained for the zirconium (8.2 kcal mol^{-1}) and hafnium complexes (8.9 kcal mol^{-1}). Following the intrinsic reaction coordinate, **TS1** led to the tetrahedral intermediate **INT1**. Rotation around the O_e−C bond afforded **INT2**, in which the O_i atom of the LA units approaches the metal (e.g., Zr····O_i = 2.308 Å). Cleavage of the six-membered heterocycle then occurred on passing through the low-lying transition state **TS2**, which comprises an eight-membered ring

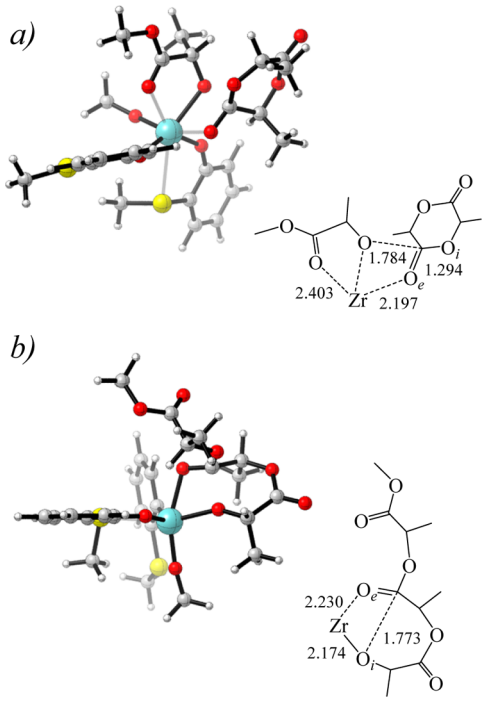

Figure 6. Transition states for the nucleophilic attack (**TS1**) and ring-opening (**TS2**) for the zirconium model complex.

with a shorter Mt−O_i distance (Zr····O_i = 2.174 Å) and a longer Mt−O_e donor interaction (Zr····O_e = 2.230 Å). This transition state led to the product **INT3** in which the monomer was fully opened (corresponding distance for zirconium based model $C_{C=O}$−O_i = 2.627 Å). Reorientation of the opened lactide molecule led to a coordination of the growing chain similar to that of the starting complex (**INT4**). The energies for the conversions of the reagents to **INT4** were slightly endothermic by −2.5, −3.3, and −4.4 kcal mol^{-1} for titanium, zirconium, and hafnium metal based model, respectively.

Our calculations suggest that the hemilability of the coordinated ligands is an indispensable prerequisite for opening a straightforward reaction pathway at the metal center. As matter of fact, the coordination of the monomer occurs through the displacement of one of the neutral sulfur donor avoiding the achievement of an improbable seven-coordination geometry. This finding could explain the higher catalytic activity of zirconium complexes with two bidentate OS ligands with respect to those of the analogous complexes with one

dx.doi.org/10.1021/ma5003358 | *Macromolecules* 2014, 47, 2830−2841

tetradentate OSSO ligand. Indeed, it can be regarded as a consequence of the lability of the sulfur donor in absence of a bridging link in the ligand framework. The increase of the catalytic activity with the increase of the flexibility of the bridge in the OSSO ligand[8] (1,2-cyclohexanediyl < 1,2-ethanediyl < 1,3-propanediyl) furnishes a further support to this hypothesis.

Polymerization of L-LA in the Presence of Isopropanol. Generally the use of alcohol in the ROP of cyclic esters offers the advantage of optimizing the productivity and minimizing the contamination of polymer with metal residues. As a matter of fact, the mole excess of alcohol can act as chain transfer agent, allowing to produce several polymer chains per metal center.[18]

Addition of isopropanol to the polymerization reaction promoted by **2** significantly affected the polymerization rate. Figure 7 reports the kinetic plots obtained in the polymerization of L-LA in the presence of 2, 5, and 10 equiv of isopropanol. With 5 equiv the activity was approximately 3 times that obtained in absence of alcohol (k_{obs} = 0.093 ± 0.004 min^{-1}). By increasing further the equivalents of isopropanol, the activity decreased. Probably the excess of alcohol reversibly coordinates to the active species leading to catalytic inhibition. A similar effect was already observed in the ROP of cyclic ester promoted by aluminum catalysts.[19] The $M_{n(expt)}$ of the resulting PLAs increased linearly with the conversion with values proportional to the equivalents of added isopropanol indicating that, under such conditions, extra polymer chains were created to the same extent as equivalents of isopropanol introduced. A strict agreement between the experimental and the theoretical values of the M_n values was also observed (Figure 8). Significantly, the PDI indexes, with values in the range 1.09−1.13, were narrower than those obtained in absence of alcohol likely as a consequence of suppressing transesterification side reactions. End-group analysis by ^{1}H NMR spectroscopy of the PLAs obtained under such conditions showed clearly that the polymer chains were systematically end-capped with an isopropyl ester and a hydroxy group. All experimental data demonstrate that adequate conditions for effective *"immortal"* polymerizations were achieved.

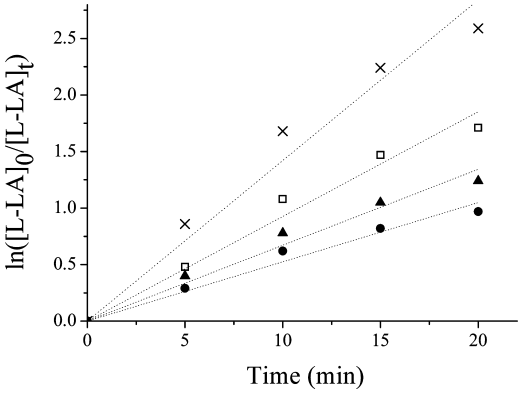

Figure 7. Pseudo-first-order kinetic plots for ROP of L-LA promoted by complexes **2** or $Zr(OtBu)_4$ in the presence of isopropanol. (●) **2**/*i*PrOH-2 equiv, k_{obs} = 0.052 ± 0.002 min^{-1}, R = 0.989; (□) **2**/*i*PrOH-5 equiv, k_{obs} = 0.093 ± 0.004 min^{-1}, R = 0.990; (▲) **2**/*i*PrOH-10 equiv, k_{obs} = 0.067 ± 0.003 min^{-1}, R = 0.989; (×) $Zr(OtBu)_4$/*i*PrOH-5 equiv, k_{obs} = 0.142 ± 0.007 min^{-1}, R = 0.986. Conditions: $[I]_0$ = 5.2 mM; $[LA]_0/[I]_0$ = 100; toluene as solvent; T = 80 °C.

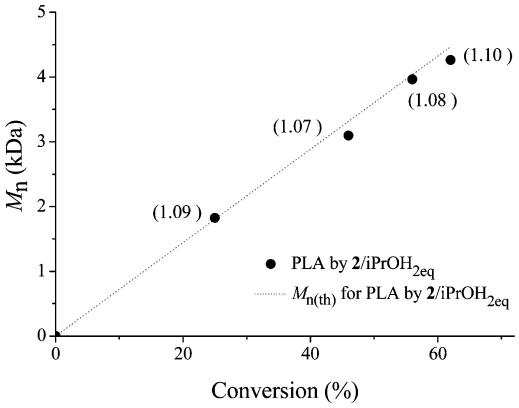

Figure 8. Plot of number-averaged molecular weights M_n vs monomer conversion using **2**/*i*PrOH for L-LA polymerization. M_w/M_n values are in parentheses. Conditions: $[I]_0$ = 5.2 mM; $[LA]_0$:$[I]_0$:[*i*PrOH] = 100:1:2; toluene as solvent; T = 100 °C.

To acquire more insight into the mechanism of the polymerization conducted in the presence of alcohol, the reaction of **2** with isopropanol was monitored by NMR spectroscopy. To our surprise, in the ^{1}H NMR spectrum the resonances of the free ligand were clearly detected indicating a partial protonolysis of complex **2**. By using 2 equiv of isopropanol, at room temperature in C_6D_6, the ratio between the free ligand and the unreacted complex was 1:2 (see Figure S14). Similar alcholysis with the release of neutral ligand were previously observed in the reaction of some metal base complexes with isopropanol or phenol to achieve an active catalytic system for the ROP of ε-caprolactone.[19d,20] The *tert*-butyl alcohol was also indentified in the reaction mixture. It is plausible to assume that the alcoholysis of complex **2** leads to the formation of the zirconium tetraisopropoxide, a dimeric alchoholate $[Zr(O\text{-}i\text{-}Pr)_4(i\text{-}PrOH)]_2$ in rapid exchange with the free alcohol.[21] In the ^{1}H NMR spectrum two multiplet at 4.57 and 4.41 ppm were detected and tentatively assigned to the methine proton of the zirconium tetraisopropoxide.

$[Zr(O\text{-}i\text{-}Pr)_4(i\text{-}PrOH)]_2$ is plausibly acting as initiators in the polymerization of L-LA. For the sake of comparison, a blank experiment conducted with $Zr(OtBu)_4$ in the presence of isopropanol was performed. To our surprise, considerable conversion was achieved within 20 min. The $Zr(O\text{-}t\text{-}Bu)_4$/*i*-PrOH catalytic system showed pseudo-first-order rate constants higher than that obtained for **2**/*i*-PrOH under the same reaction conditions (0.142 ± 0.007 min^{-1} vs 0.093 ± 0.004 min^{-1}, Figure 7). The molecular weight increased monotonously with conversion (see Figure S15), but the PDI were slightly higher than those observed for **2**/*i*-PrOH. The $Zr(O\text{-}t\text{-}Bu)_4$/*i*-PrOH catalytic system showed performances quite different from those observed for **2**/*i*-PrOH under the same reaction conditions. Although the nature of the active species produced in the reaction between **2** and *i*-PrOH is still unclear and deserve further investigations, it is evident that the ligands used herein play an important role in the formation of the active species which efficiently initiated the ROP polymerization of L-LA in a controlled manner.

Ring-Opening Polymerization of ε-Caprolactone. Group 4 metal complexes **1**−**4** were also assessed in the ring-opening polymerization of ε-caprolactone (CL). Polymerizations were carried out in toluene solution at 80 °C with a prescribed equivalent molar ratio of initiator and monomer. The polymerization runs were tracked by analyzing the product

dx.doi.org/10.1021/ma5003358 | Macromolecules 2014, 47, 2830−2841

Table 2. Ring-Opening Polymerization of L-LA Initiated by 2 or $Zr(OtBu)_4$ in the Presence of *i*PrOH

entry[a]	complex	[iPrOH]/[I]	*t*/min	conv/%[b]	$M_{n(th)}$[c]	$M_{n(GPC)}$[d]	PDI[d]
1	**2**	2	20	62	4468	4262	1.10
2	**2**	5	20	82	2364	3096	1.09
3	**2**	10	20	71	1023	1457[e]	–
4	$Zr(OtBu)_4$	5	20	92	2666	2325	1.22

[a]All reactions were carried out in 2.4 mL of toluene, $[I]_0$ = 5.2 mM, [LA] = 0.52 M, $[LA]/[I]_0$ = 100, polymerization temperature 80 °C. [b]Molecular conversion determined by ^{1}H NMR spectroscopy ($CDCl_3$, 298 K). [c]Calculated molecular weight using $M_{n,th}$ (kg mol^{-1}) = 144.13 × ($[LA]_0$/$[i\text{PrOH}]_0$) × LA conversion. [d]Experimental molecular weight M_n (kg mol^{-1}) and polydispersity (PDI) determined by GPC in THF using polystyrene standards and corrected using a factor of 0.58. [e]Experimental molecular weight determined by ^{1}H NMR from the relative intensities of the main chain and the terminal resonances.

mixtures sampled from the reactor at certain reaction times. The main results of the polymerization studies are summarized in Table 3.

Table 3. Ring-Opening Polymerization of ε-Caprolactone by 1−4

entry[a]	initiator	*t*/min	conv/%[b]	$M_{n,th}$[c]	$M_{n,GPC}$[d]	PDI[d]
1	**1**	75	96	6.9[e]	6.0	1.25
2	**2**	75	94	13.5	29.9	1.40
3	**3**	90	93	13.5	34.1	1.29
4	**4**	120	73	10.5	13.9	1.27

[a]All reactions were carried out in 2.4 mL of toluene, $[I]_0$ = 5.2 mM, [CL] = 0.52 M, $[CL]/[I]_0$ = 100, polymerization temperature 80 °C. [b]Molecular conversion determined by ^{1}H NMR spectroscopy ($CDCl_3$, 298 K). [c]Calculated molecular weight using $M_{n,th}$ (kg mol^{-1}) = 114.14 × ($[CL]_0/[I]_0$) × CL conversion. [d]Experimental molecular weight M_n (kg mol^{-1}) and polydispersity (PDI) determined by GPC in THF using polystyrene standards and corrected using a factor of 0.56. [e]$M_{n,th}$ (kg mol^{-1}) = 114.14 × ($[CL]_0/[2 \times I]_0$) × CL conversion.

Complexes **1**−**3** showed good productivities, reaching high conversions of 100 equiv of CL in about 75 min. Complex **4** was less active, allowing good conversion only after 2 h of reaction. In this polymerization the presence of the sterically encumbered cumyl group in the *ortho* position of the aromatic ring had a detrimental effect on the catalytic activity. In all cases, the polymerization followed first-order kinetics in the concentration of CL (Figure 9). The kinetic constants were

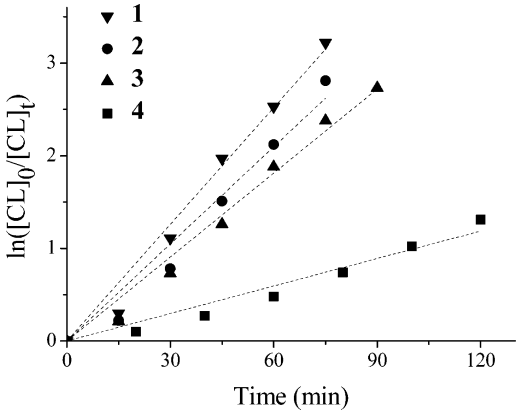

Figure 9. Pseudo-first-order kinetic plots for ROP of ε-CL promoted by complexes **1**−**4**. The pseudo-first-order rate constants are k_{obs}(**1**) = 0.042 ± 0.001 min^{-1} (R = 0.992), k_{obs}(**2**) = 0.035 ± 0.002 min^{-1} (R = 0.984), k_{obs}(**3**) = 0.030 ± 0.001 min^{-1} (R = 0.993), and k_{obs}(**4**) = 0.0099 ± 0.0005 min^{-1} (R = 0.982). Conditions: $[I]_0$ = 5.2 mM; $[CL]_0/[I]_0$ = 100; toluene as solvent; T = 80 °C.

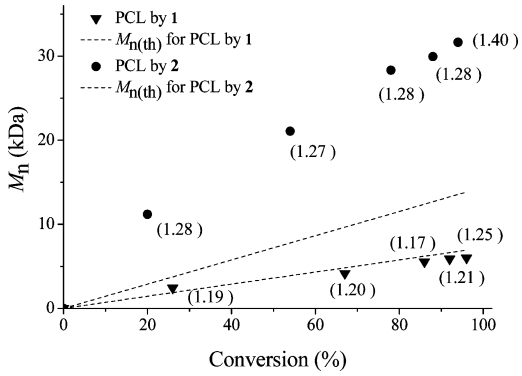

Figure 10. Plots of number-averaged molecular weights M_n vs monomer conversion (%) with theoretical $M_{n(th)}$ for the polymerization of ε-CL using **1** and **2** as an initiator. Conditions: $[I]_0$ = 5.2 mM, $[CL]_0/[I]_0$ = 100, toluene, 80 °C; polydispersities shown in parentheses.

0.042 ± 0.001, 0.035 ± 0.002, 0.030 ± 0.001, and 0.0099 ± 0.0005 min^{-1} for **1**, **2**, **3**, and **4**, respectively. The linearity of the plot showed that the propagation was first order with respect to monomer. All polymerizations led to polymers with monomodal and narrow molecular weight distributions. The experimental number-average molecular weight increased linearly with the increase in the monomer conversion. As already observed in the polymerization of L-lactide, the molecular weights of the polymer obtained by **1** showed a good agreement with the theoretical molecular weights calculated assuming the growth of two polymer chains per Ti initiator. Differently the molecular weights of the PCL by **2**−**4** were significantly higher than those calculated assuming the growth of one polymer chain for metal center (Figure 10). This suggested that, possibly, only a fraction of metal complex was involved in catalysis, most likely as a result of an inefficient initiation and rapid propagation.

The ^{1}H NMR spectra of the PCL samples obtained from the polymerizations initiated by **1** featured the expected resonances attributable to the of isopropyl ester end groups (COOCH-$(CH_3)_2$; 5.03 and 1.24 ppm) and hydroxyl end groups (CH_2CH_2OH; 3.61 ppm). The observation of these end groups suggests that a coordination−insertion mechanism should be operative.

Copolymerization of L-Lactide and ε-Caprolactone. In order to further explore the catalytic ability of this class of complexes, we investigated the performances of titanium and zirconium complexes **1** and **2** in the random CL/L-LA copolymerization. Copolymerization tests were carried out by using 100 equiv of both monomers in toluene solution at 100 °C. Complexes **1** and **2** resulted excellent catalysts for the

dx.doi.org/10.1021/ma5003358 | Macromolecules 2014, 47, 2830−2841

synthesis of these copolymers, providing polymers with monomodal molecular weight distributions (PDI(**1**) = 1.41; PDI(**2**) = 1.48). In both cases the percent conversion of lactide was high (99%), while the percent conversion of ε-caprolactone was 64%. In both cases the mole fraction of LA and CL in the polymer was similar to that in the feed: [LA]/[CL] was 58/42 and 52/48 for **1** and **2**, respectively. The chain microstructures of the copolymers were investigated by ^{13}C NMR spectroscopy in the carbonyl region of the spectra (Figure 11). All peaks due

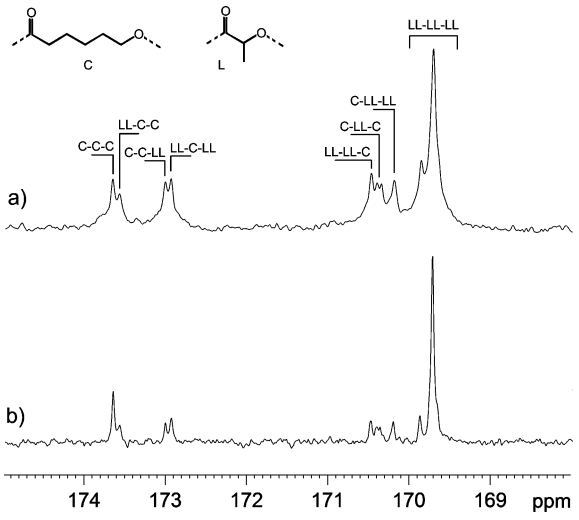

Figure 11. Carbonyl region of ^{13}C NMR spectra ($CDCl_3$, 25 °C) of copolymers obtained by **1** (a) and **2** (b).

to the different monomer sequences in the copolymer were observed. The average lengths of the blocks of the caproyl (L_{CL}) and lactidyl (L_{LA}) sequences were 1.7 and 2.9 for the copolymer by **1** and 4.2 and 2.5 for the copolymer by **2** (an ideal random copolymer will have $L_{LA} = L_{CL} = 2$). Recently random copolymers were obtained in the presence of bis(pyridonate)− and bis(amidate)−titanium complexes, reported as rare examples of titanium based catalysts capable of producing random copolymer.[22] The thermal properties of the copolymers were analyzed by differential scanning calorimetry. The copolymers resulted amorphous and displayed a unique glass transition temperature intermediate between those of the corresponding homopolymers (T_g(copol by **1**) = −2 °C, T_g(copol by **2**) = 5 °C, T_g(PCL) = −60 °C, T_g(PLA) = 57 °C). The microstructure disclosed by ^{13}C NMR analysis and the thermal behavior exhibited in DSC studies support a structure for the obtained copolymer that is very close to a random distribution of the two monomer along the polymer.

CONCLUSIONS

New group 4 metal complexes supported by two bidentate thioetherphenolate ligands were successfully synthesized via alcohol elimination reaction and characterized by NMR spectroscopy and X-ray diffraction studies. All complexes exhibited an octahedral geometry in which the two OS^- ligands are κ^2-coordinated to the metal center in a α-cis configuration. The complexes were conformationally flexible; as matter of fact, solution-state NMR spectroscopic measurements revealed that a fast fluxional process is active involving the inversion of configuration at the metal center.

All the complexes acted as efficient initiators for the ring-opening polymerization of L- and *rac*-lactide, affording PLAs with predicted molecular weights and narrow molecular weight distributions. The steric bulk of the substituents on the aromatic rings, and particularly the *o*-phenolate substituents, played a crucial role in achieving high activity. The zirconium complex with the cumyl groups on the ligand skeleton displayed the highest activity among this class of complexes. The activity of complex $(^{Cum}OS)_2Zr(O\text{-}t\text{-}Bu)_2$ compares favorably with those of the most active group 4 complexes reported so far for the polymerization of lactide. A DFT study on the ROP mechanism evidenced the importance of the hemilability of the ancillary ligand during the polymerization reaction. It was shown that the κ^1 coordination is an indispensable prerequisite for coordination of the monomer and for opening a straightforward reaction pathways at the metal center. Upon addition of isopropanol, efficient binary catalytic system for the "*immortal*" ring-opening polymerization was produced. Although the effect of alcohol deserves further investigations, it was evident that the ligands used herein play an important role in the formation of the active species. The loss of control at high monomer to initiator ratio and the poor stereoselectivity for ROP of *rac*-lactide limit the potential usefulness of these complexes. This notwithstanding, the performances displayed by these catalysts may encourage the design and preparation of new series of low cost and nontoxic group 4 metal complexes for the ring-opening polymerization of cyclic esters.

Furthermore, titanium and zirconium complexes turned out to be very efficient initiators for copolymerization of caprolactone with lactide. Although homopolymerization rates of lactide and caprolactone were substantially different, random copolymers of L-LA and CL were easily prepared by mixing the two monomers in appropriate proportion. To the best of our knowledge, these complexes are among the rare examples of discrete group 4 complexes able to produce random copolymers of L-lactide with ε-caprolactone.

GENERAL PROCEDURES

All experiments that required inert atmosphere were performed under nitrogen using a Braun Labmaster drybox or standard Schlenk line techniques. Solvents were distilled over sodium (toluene), sodium/benzophenone/diglyme (hexane, pentane), or $LiAlH_4$ (diethyl ether). When not pointed out the reagents were used as received from the supplier (Sigma-Aldrich). Ligands used for the synthesis of the complexes were anhydrificated in vacuum with P_2O_5. ε-Caprolactone (CL) was distilled over CaH_2. Lactide was purified by crystallization from dry toluene and then stored over P_2O_5. 2-Propanol was purified by distillation over sodium.

Instruments and Measurements. NMR spectra were recorded on a Bruker AM300 and Bruker AVANCE 400 operating at 300.13 and 400.13 MHz for ^{1}H, respectively. Deuterated solvents were purchased from Cambridge Isotope Laboratories, Inc., degassed, and dried over activated 4 Å molecular sieves prior to use. Chemical shifts (δ) are listed as parts per million and coupling constants (J) in hertz. ^{1}H NMR spectra are referenced using the residual solvent peak at δ 7.16 for C_6D_6, δ 5.32 for CD_2Cl_2, and δ 7.27 for $CDCl_3$. ^{13}C NMR spectra are referenced using the residual solvent peak at δ 128.39 for C_6D_6, δ 53.84 for CD_2Cl_2, and δ 77.23 for $CDCl_3$. Variable-temperature ^{1}H NMR experiments were recorded with a Bruker Avance 400 spectrometer in CD_2Cl_2 using J-Young NMR tube. In the case of polylactide samples obtained from the polymerization of *rac*-LA, the evaluation of the probability to obtain an *r* diad (P_r) was made by the analysis of the relative intensities of the tetrads signals of the ^{1}H NMR homonuclear decoupled spectrum ($CDCl_3$, 300 MHz, ppm): *mrm* (5.16), *mmm* (5.17), *mmr*/*rmm* (5.18 and 5.22), and *rmr* (5.23).[23] Electrospray ionization mass spectra were acquired using a

dx.doi.org/10.1021/ma5003358 | *Macromolecules* 2014, 47, 2830−2841

Micromass Quattro micro API triple quadrupole mass spectrometer equipped with an electrospray ion source (Waters, Milford, MA). Acetonitrile was added to the samples, and the solutions were continuously infused into the electrospray ionization (ESI) ion source at a rate of 10 μL/min using the instrument syringe pump. The LCQ ion source was operating at 4 kV, and the capillary heater was set to 100 °C. Nitrogen was used as nebulizing gas, and nitrogen was used as damping gas and collision gas in the mass analyzer. Positive ion mode was used for all analyses. No cationizing agents were used for ESI measurements because K^+, Na^+, and H^+ adduct ions were detectable at high intensity. The origin of these alkali metals was apparently the ambient contaminants. The molecular weights (M_n and M_w) and the molecular weights distributions (M_w/M_n) of polymer samples were measured by gel permeation chromatography (GPC) at 30 °C using THF as the solvent, a flow rate of the eluent of 1 mL/min, and narrow polystyrene standards as the references. The measurements were performed on a Waters 1525 binary system equipped with a Waters 2414 RI detector using four Styragel columns (range 1000−1 000 000 Å). The values were corrected using the factor 0.58 for polylactide and 0.56 for polycaprolactone according to the literature.[24] Glass transition temperatures (T_g) and melting points (T_m) of the polymers were measured by differential scanning calorimetry (DSC) using a DSC 2920 (TA Instruments) in nitrogen flow with a heating and cooling rate of 10 °C min^{-1} in the range −100 to 200 °C. Glass transition temperatures and melting temperatures were reported for the second heating cycle.

Synthesis of Ligands. The 4,6-di-*tert*-butyl-2-phenylsulfanylphenol proligand ($^{t\text{-Bu}}$OS-H) was synthesized according to the previously reported procedures.[9] Spectroscopic data: ^{1}H NMR (300.13 MHz, $CDCl_3$, 25 °C): δ 1.28 (9H, s); 1.40 (9H, s); 6.83 (1H, s, −OH); 7.00−7.45 (7H, Ar−H). ^{13}C NMR (75.47 MHz, $CDCl_3$, 25 °C): δ 29.57; 31.67; 34.54; 35.44; 115.68; 125.88; 126.44; 127.02; 129.26; 131.22; 135.89; 136.60; 142.94; 153.58.

Synthesis of 2-Bromo-4,6-bis(α,α-dimethylbenzyl)phenol. In a round-bottomed flask, equipped with a magnetic stirrer, CH_2Cl_2 (200 mL), 4,6-bis(α,α-dimethylbenzyl)phenol (25.6 g, 73.6 mmol), and bromine (4.0 mL, 77.4 mmol) were added in sequence. After stirring for 1 h, the reaction mixture was extracted with water (2 × 100 mL), anhydrificated with Na_2SO_4, and the solvent was removed in vacuum. The desired product was collected as a pale yellow solid (26.5 g, 64.7 mmol, yield 88%). Spectroscopic data: ^{1}H NMR (300.13 MHz, $CDCl_3$, 25 °C): δ 1.62 (6H, s); 1.70 (6H, s); 5.17 (1H, s, −OH); 7.10−7.40 (15H, Ar−H). ^{13}C NMR (75.47 MHz, $CDCl_3$, 25 °C) δ: 29.53; 31.08; 42.79; 111.84; 125.46; 125.84; 125.93; 126.05; 126.82; 128.23; 128.48; 128.86; 136.26; 143.62; 148.09; 149.51; 150.42.

Synthesis of Phenylsulphenyl Chloride.[25] In a round-bottomed flask, equipped with a magnetic stirrer, CH_2Cl_2 (90 mL) and thiophenol (18.5 mL, 0.18 mol) were added under an inert atmosphere. Sulfuryl chloride, SO_2Cl_2 (14.6 mL, 0.18 mol), was added dropwise at 0 °C. After the addition, the mixture was stirred for 1 h, and the solvent was removed in a vacuum. The product was recovered as a red oil and stored under nitrogen in the absence of light.

Synthesis of 4,6-Bis(α,α-dimethylbenzyl)-2-phenylsulfanylphenol (^{Cum}OS-H). In a round-bottomed flask, equipped with a magnetic stirrer, dry THF (50 mL) and 2-bromo-4,6-bis(α,α-dimethylbenzyl)-phenol (8.19 g, 20.0 mmol) were added under an inert atmosphere. After cooling the system to −50 °C, 1 equiv of butyllithium (8.0 mL, 2.5 M in hexane) was added dropwise. After 10 min, a second equivalent of butyllithium was added dropwise (8.0 mL, 2.5 M in hexane). The temperature was slowly raised to room temperature and the mixture stirred for 30 min. The system was cooled to −65 °C, and phenylsulfenyl chloride in THF) (50 mL, 0.40 M) was added dropwise. The mixture was stirred for 12 h; during this time the temperature was slowly increased to room temperature. Distilled water (25 mL) was added to the mixture under stirring. The organic phase was extracted with THF (2 × 25 mL) and CH_2Cl_2 (50 mL). The unified organic phases were anhydrificated with Na_2SO_4, and the solvent was removed in vacuum. The product was purified by column chromatography (eluent hexane:ethyl acetate 98:2). Yield 5.9 g (67%). Spectroscopic data: ^{1}H NMR (300.13 MHz, $CDCl_3$, 25 °C): δ 1.66 (6H, s); 1.72 (6H, s); 6.35 (1H, s, −OH); 6.91 (1H, m, Ar−H); 6.94 (1H, m, Ar−H); 7.10−7.40 (15H, Ar−H). ^{13}C NMR (75.47 MHz, $CDCl_3$, 25 °C): δ 29.50; 31.08; 42.62; 42.81; 116.44; 125.51; 125.70; 125.83; 126.56; 126.81; 128.04; 128.17; 128.68; 129.13; 132.83; 135.43; 136.27; 142.61; 150.38; 150.72; 153.12.

Synthesis of ($^{t\text{-Bu}}$OS)$_2$Ti(O-*i*-Pr)$_2$ (1). A solution of Ti(O-*i*-Pr)$_4$ (0.373 g, 1.31 mmol) in toluene (5 mL) was added to a stirred solution of $^{t\text{-Bu}}$OS-H (0.824 g, 2.61 mmol) in toluene (15 mL) at room temperature. The resulting pale yellow solution was stirred for 1 h, after which the volatiles were removed in a vacuum. The crude product was washed with hexane to give **1** as a yellow solid (0.686 g, 66%). Spectroscopic data: ^{1}H NMR (300.13 MHz, C_6D_6, 25 °C): δ 1.17 (12H, d); 1.28 (18H, s); 1.86 (18H, s); 4.58 (2H, m); 6.83−7.68 (14H, Ar−H). ^{13}C NMR (75.47 MHz, C_6D_6, 25 °C): δ 26.32; 30.47; 32.06; 34.81; 36.29; 80.88; 119.70; 126.11; 126.25; 127.64; 129.06; 130.26; 137.36; 139.12; 142.25; 163.35. Elemental analysis calcd (%) for $C_{46}H_{64}O_4S_2Ti$: C, 69.67; H, 8.13; S, 8.09. Found C, 69.75; H, 8.24; S, 8.01.

Synthesis of ($^{t\text{-Bu}}$OS)$_2$Zr(O-*t*-Bu)$_2$ (2). A solution of Zr(O-*t*-Bu)$_4$ (1.58 mmol, 0.6069 g) in toluene (5 mL) was added to a stirred solution of $^{t\text{-Bu}}$OS-H (3.16 mmol, 0.993g) in toluene (15 mL) at room temperature. The resulting pale yellow solution was stirred for 1 h, after which the volatiles were removed in vacuum. The crude product was washed with hexane to give **2** as a yellow solid (0.915 g, 67%). Single crystals of the complex were grown from cold pentane. Spectroscopic data: ^{1}H NMR (300.13 MHz, C_6D_6, 25 °C): δ 1.19 (18H, s); 1.22 (18H, s); 1.77 (18H, s); 6.73−7.60 (14H, Ar−H). ^{13}C NMR (75.47 MHz, C_6D_6, 25 °C): δ 29.91; 31.73; 32.57; 34.43; 35.99; 77.76; 118.28; 126.12; 126.39; 127.23; 129.01; 129.58; 137.01; 138.11; 141.21; 164.35. Elemental analysis calcd (%) for $C_{48}H_{68}O_4S_2Zr\cdot 0.5C_5H_{12}$: C, 67.36; H, 8.28; S, 7.12. Found C, 67.54; H, 8.32; S, 7.26.

Synthesis of ($^{t\text{-Bu}}$OS)$_2$Hf(O-*t*-Bu)$_2$ (3). A solution of Hf(O-*t*-Bu)$_4$ (0.373 g, 7.93 × 10^{-1} mmol) in toluene (5 mL) was added to a stirred solution of $^{t\text{-Bu}}$OS-H (0.499 g, 1.58 mmol) in toluene (10 mL) at room temperature. The resulting pale yellow solution was stirred for 1 h, after which the volatiles were removed in a vacuum. The crude product was washed with hexane to give **3** as a yellow solid (0.394 g, 52%). Spectroscopic data: ^{1}H NMR (300.13 MHz, C_6D_6, 25 °C): δ 1.19 (18H, s); 1.23 (18H, s); 1.78 (18H, s); 6.70−7.60 (14H, Ar−H). ^{13}C NMR (75.47 MHz, C_6D_6, 25 °C): δ 30.27; 32.07; 33.13; 34.75; 36.29; 77.59; 118.14; 126.56; 126.86; 127.72; 129.32; 129.93; 137.25; 139.33; 141.55; 165.11. Elemental analysis calcd (%) for $C_{48}H_{68}HfO_4S_2$: C, 60.58; H, 7.20; S, 6.74. Found C, 60.67; H, 7.36; S, 6.87.

Synthesis of (^{Cum}OS)$_2$Zr(O-*t*-Bu)$_2$ (4). A solution of Zr(O-*t*-Bu)$_4$ (0.318 g, 8.3 × 10^{-1} mmol) in toluene (5 mL) was added to a stirred solution of ^{Cum}OS-H (0.727g, 1.66 mmol) in toluene (10 mL) at room temperature. The resulting pale yellow solution was stirred for 1 h, after which the volatiles were removed in a vacuum. The crude product was washed with hexane to give **4** as a yellow solid (0.333 g, 36%). Spectroscopic data: ^{1}H NMR (300.13 MHz, C_6D_6, 25 °C): δ 1.01 (18H, s); 1.52 (12H, s); 1.88 (12H, s, broad); 6.7−7.6 (34H, Ar−H). ^{13}C NMR (75.47 MHz, C_6D_6, 25 °C): δ 30.99; 31.40; 32.41; 32.54; 42.69; 43.16; 77.78; 118.56; 125.38; 125.86; 126.30; 126.41; 127.01; 127.29; 128.16; 128.28; 128.92; 130.80; 131.50; 136.86; 137.67; 140.47; 151.28; 164.15. Elemental analysis calcd (%) for $C_{58}H_{72}O_4S_2Zr$: C, 70.47; H, 7.34; S, 6.49. Found C, 70.56; H, 7.48; S, 6.62.

Lactide Polymerizations. In a typical polymerization, in a glovebox, a Schlenk flask (10 cm^3) was charged sequentially with the monomer (*rac*- or L-lactide, 0.180 g, 1.25 mmol), and a solution of catalyst (12.5 μmol in 2.4 mL of dry toluene). The mixture was thermostated at the required temperature. At specified time intervals, a small amount of the polymerization mixture was sampled by a pipet and quenched in wet $CDCl_3$. This fraction was subjected to monomer conversion determination, which was monitored by integration of monomer versus polymer methine resonances in ^{1}H NMR spectrum ($CDCl_3$). After the required polymerization time, the reaction mixture was quenched with wet *n*-hexane. The precipitates collected from the

dx.doi.org/10.1021/ma5003358 | Macromolecules 2014, 47, 2830−2841

bulk mixture were dried in air, dissolved with dichloromethane, and sequentially precipitated into methanol. The obtained polymer was collected by filtration and further dried in a vacuum oven at 40 °C for 16 h. The polymer was characterized by NMR spectroscopy and GPC analysis. The chemical shifts of polylactide are 1.64 (d, 6H, $-CHCH_3-$) and 5.18 (q, 2H, $-CHCH_3-$). The chemical shifts of lactide are 1.59 (d, 6H, $-CHCH_3-$) and 4.85 (t, 2H, $-CHCH_3-$).

Lactide Polymerizations in the Presence of Isopropanol. In a typical polymerization, in a glovebox, a Schlenk flask (10 cm^3) was charged sequentially with L-lactide (0.180 g, 1.25 mmol), and a solution of catalyst (12.5 μmol in a proper amount of dry toluene to reach a total volume of 2.4 mL). Subsequently, 0.30, 0.75, or 1.5 mL of a 0.083 M solution of isopropanol in toluene (25, 62.5, or 125 μmol) was added. The volume was kept constant to 2.4 mL. The mixture was thermostated at the required temperature. At specified time intervals, a small amount of the polymerization mixture was sampled by a pipet and quenched in wet $CDCl_3$. This fraction was subjected to monomer conversion determination, which was monitored by integration of monomer versus polymer methine resonances in ^1H NMR spectrum ($CDCl_3$). After the required polymerization time, the reaction mixture was quenched with wet *n*-hexane. The precipitates collected from the bulk mixture were dried in air, dissolved with dichloromethane, and sequentially precipitated into methanol. The obtained polymer was collected by filtration and further dried in a vacuum oven at 40 °C for 16 h. The polymer was characterized by NMR spectroscopy and GPC analysis.

ε-Caprolactone Polymerization. In a typical polymerization, a Schlenk flask (10 cm^3) was charged sequentially with a solution of the catalyst (12.5 μmol in 2.4 mL of dry toluene) and the monomer (0.14 mL, 1.25 mmol). The mixture was thermostated at the required temperature. At specified time intervals, a small amount of the polymerization mixture was sampled by a pipet and quenched in wet $CDCl_3$. This fraction was subjected to monomer conversion determination, which was monitored by integration of monomer versus polymer methylene resonances in ^1H NMR spectrum ($CDCl_3$). After the required polymerization time, the reaction mixture was quenched with wet *n*-hexane. The precipitates collected from the bulk mixture were dried in air, dissolved with dichloromethane, and sequentially precipitated into methanol. The obtained polymer was collected by filtration and further dried in a vacuum oven at 40 °C for 16 h. The polymer was characterized by NMR spectroscopy and GPC analysis. The polymer was characterized by NMR spectroscopy and GPC analysis. The chemical shifts of polycaprolactone are 1.34 (m, 2H, $-CH_2-$), 1.62 (m, 4H, $-CH_2-$), 2.29 (t, 2H, $-CH_2CH_2C{=}O$), and 4.04 (t, 2H, $-OCH_2CH_2-$). The chemical shifts of ε-caprolactone are 0.98 (4H, m, $-CH_2-$), 1.12 (2H, m, $-CH_2-$), 2.09 (2H, t, $-CH_2CH_2C{=}O$), and 3.46 (2H, t, $-OCH_2CH_2-$).

Synthesis of Poly(ε-caprolactone-*co*-L-lactide). A Schlenk tube equipped with a magnetic stirrer was charged sequentially with L-lactide (0.180 g, 1.25 mmol), ε-caprolactone (0.14 mL, 1.25 mmol), and the catalyst (12.5 μmol) dissolved in 2.4 mL of dry toluene. The mixture was thermostated at 100 °C. After the required polymerization time, an aliquot of the crude material was sampled by a pipet and quenched in wet $CDCl_3$ to evaluate the yields. Conversions were determined by integration of the monomer vs polymer resonances in the ^1H NMR spectrum of the crude product (in $CDCl_3$). The reaction mixture was quenched with wet *n*-hexane. The precipitates collected from the bulk mixture were dried in air, dissolved with dichloromethane, and sequentially precipitated into methanol. The obtained polymer was collected by filtration and further dried in a vacuum oven at 40 °C for 16 h. The polymer was characterized by NMR spectroscopy, GPC, and DSC analysis.

Computational Details. Density functional theory (DFT) calculations were performed with the program suite Gaussian 09.[26] All geometries were optimization without constraints at the BP86 level, i.e., employing the exchange and correlation functionals of Becke and Perdew,[27] respectively. The basis set employed was the LANL2DZ[28] with associate effective core potentials for Ti, Zr, Hf, and S and the SVP[29] for O, C, and H. To save computational resources, the bulky alkyl substituents were removed and the phenyl groups bound to the sulfur atom were replaced with methyl groups; the growing chain was modeled by a metal-(*S*)-methyl-lactate.[30] Geometry optimizations were performed without symmetry constraints. Stationary point geometries were characterized as local minimum on the potential energy surfaces. The absence of imaginary frequency verified that structures were true minima at their respective levels of theory. The structure of transition state were located by applying Schlegel's synchronous-transit-guided quasi-Newton (QST2) method as implemented in GAUSSIAN 09. The transition states were verified with frequency calculations to ensure they were first-order saddle points with only one negative eigenvalue. Cartesian coordinates of all DFT optimized structures are available on request. Structures were visualized by the CYLview program.[31]

Single Crystal X-ray Crystallography. Single crystals of **2** suitable for X-ray analysis were obtained from an *n*-pentane solution at 253 K. Data collection was performed in flowing N_2 at 173 K on a Bruker-Nonius kappaCCD diffractometer (Mo Kα radiation, CCD rotation images, thick slices, φ scans + ω scans to fill the asymmetric unit). Cell parameters were determined from 169 reflections in the range $3.059° \leq \theta \leq 19.255°$. Semiempirical absorption corrections (multiscan SADABS)[32] were applied. The structure was solved by direct methods (SIR 97 package)[33] and refined by the full matrix least-squares method (SHELXL program of SHELX97 package)[34] on F^2 against all independent measured reflections, using anisotropic thermal parameters for all non-hydrogen atoms. H atoms, except for the disordered solvent molecule, were placed in calculated positions with U_{eq} equal to those of the carrier atom and refined by the riding method. All plots were generated by using the program ORTEP-3.[35] Crystal data and details of the data collections are reported in Table S1 of the Supporting Information. Crystallographic data for the structural analysis have been deposited with the Cambridge Crystallographic Data Center, CCDC No. 977016. Copies of this information may be obtained free of charge from the Director, CCDC, 12, Union Road, Cambridge CB2 1EZ [Fax +44(1223)336-033] or e-mail deposit@ccdc.cam.ac.uk or http://www.ccdc.cam.ac.uk.

■ ASSOCIATED CONTENT

Supporting Information

Figures giving ^1H NMR spectra of complexes **1**−**4**, plots of number-averaged molecular vs monomer conversion, pseudo-first-order kinetic plots, and crystallographic data for complex **2**. This material is available free of charge via the Internet at http://pubs.acs.org.

■ AUTHOR INFORMATION

Corresponding Author

*E-mail: smilione@unisa.it (S.M.).

Notes

The authors declare no competing financial interest.

■ ACKNOWLEDGMENTS

The authors thank Dr. Patrizia Oliva for NMR assistance and Dr. Ilaria D'Auria for GPC measurements. For the financial support of this research the Universita' degli Studi di Salerno (FARB 2012), Ministero dell'Universita' e della Ricerca Scientifica (MIUR, Roma, Italy; PRIN-2010: "Materiali Polimerici Nanostrutturati con strutture molecolari e cristalline mirate, per tecnologie avanzate e per l'ambiente"), and Regione Campania (POR CAMPANIA Rete di Eccellenza FSE. Progetto "MAteriali e STrutture Intelligenti", MASTRI, Codice 4-17-3, CUP B25B09000010007) are gratefully acknowledged.

■ DEDICATION

This paper is dedicated to Prof. Adolfo Zambelli on the occasion of his 80th birthday.

REFERENCES

(1) Chen, G.-Q.; Patel, M. K. *Chem. Rev.* **2012**, *112*, 2082−2099.

(2) (a) Mecking, S. *Angew. Chem., Int. Ed.* **2004**, *43*, 1078−1085. (b) Ragauskas, A. J.; Williams, C. K.; Davison, B. H.; Britovsek, G.; Cairney, J.; Eckert, C. A.; Frederick, W. J., Jr.; Hallett, J. P.; Leak, D. J.; Liotta, C. L.; Mielenz, J. R.; Murphy, R.; Templer, R.; Tschaplinski, T. *Science* **2006**, *311*, 484−489. (c) Tschan, M. J.-L.; Brulé, E.; Haquette, P.; Thomas, C. M. *Polym. Chem.* **2012**, *3*, 836−851. (d) Robert, C.; de Montigny, F.; Thomas, C. M. *Nat. Commun.* **2011**, *2*, 586−592.

(3) (a) Albertsson, A.-C.; Varma, I. K. *Adv. Polym. Sci.* **2002**, *157*, 1−40. (b) Albertsson, A.-C.; Varma, I. K. *Biomacromolecules* **2003**, *4*, 1466−1486. (c) Ha, C. S.; Gardella, J. A. *Chem. Rev.* **2005**, *105*, 4205−4232. (d) Auras, R.; Harte, B.; Selke, S. *Macromol. Biosci.* **2004**, *4*, 835−864.

(4) (a) Dubois, P.; Coulembier, O.; Raquez, J.-M. *Handbook of Ring-Opening Polymerization*; Wiley-VCH: Weinheim, 2009. (b) Dechy-Cabaret, O.; Martin-Vaca, B.; Bourissou, D. *Chem. Rev.* **2004**, *104*, 6147−6176.

(5) Sauer, A.; Kapelski, A.; Fliedel, C.; Dagorne, S.; Kol, M.; Okuda, J. *Dalton Trans.* **2013**, *42*, 9007−9023.

(6) (a) Mazzeo, M.; Lamberti, M.; D'Auria, I.; Milione, S.; Peters, J. C.; Pellecchia, C. *J. Polym. Sci., Part A: Polym. Chem.* **2010**, *48*, 1374−1382. (b) D'Auria, I.; Mazzeo, M.; Pappalardo, D.; Lamberti, M.; Pellecchia, C. *J. Polym. Sci., Part A: Polym. Chem.* **2011**, *49*, 403−413. (c) D'Auria, I.; Lamberti, M.; Mazzeo, M.; Milione, S.; Roviello, G.; Pellecchia, C. *Chem.—Eur. J.* **2012**, *18*, 2349−2360. (d) Lamberti, M.; D'Auria, I.; Mazzeo, M.; Milione, S.; Bertolasi, V.; Pappalardo, D. *Organometallics* **2012**, *31*, 5551−5560. (e) Milione, S.; Grisi, F.; Centore, R.; Tuzi, A. *Organometallics* **2006**, *25*, 266−274. (f) Silvestri, A.; Grisi, F.; Milione, S. *J. Polym. Sci., Part A* **2010**, 3632−3639. (g) Mazzeo, M.; Tramontano, R.; Lamberti, M.; Pilone, A.; Milione, S.; Pellecchia, C. *Dalton Trans.* **2013**, *42*, 9338−9351. (h) Pilone, A.; Lamberti, M.; Mazzeo, M.; Milione, S.; Pellecchia, C. *Dalton Trans.* **2013**, *42*, 13036−13047. (i) D'Auria, I.; Lamberti, M.; Mazzeo, M.; Milione, S.; Pellecchia, C. *J. Polym. Sci., Part A: Polym. Chem.* **2014**, *1*, 49−60.

(7) Sergeeva, E.; Kopilov, J.; Goldberg, I.; Kol, M. *Inorg. Chem.* **2010**, *49*, 3977−3979.

(8) (a) Buffet, J.-C.; Okuda, J. *Chem. Commun.* **2011**, *47*, 4796−4798. (b) Buffet, J.-C.; Martin, A. N.; Kol, M.; Okuda, J. *Polym. Chem.* **2011**, *2*, 2378−2384.

(9) Kruse, T.; Weyhermüller, T.; Wieghardt, K. *Inorg. Chim. Acta* **2002**, *331*, 81−89.

(10) (a) Bradley, D. C.; Mehrotra, R. C.; Gaur, D. P. *Metal Alkoxides*; Academic Press: New York, 1978. (b) Bradley, D. C.; Mehrotra, R. M.; Rothwell, I. P.; Singh, A. *Alkoxo and Aryloxo Derivatives of Metals*; Academic Press: London, 2001. (c) Mehrotra, R. M.; Singh, A. *Prog. Inorg. Chem.* **1997**, *46*, 239−454. (d) Hubert-Pfalzgraf, L. G. *Coord. Chem. Rev.* **1998**, *967*, 178−180.

(11) (a) Capacchione, C.; Proto, A.; Ebeling, H.; Mülhaupt, R.; Spaniol, T. P.; Möller, V.; Okuda, J. *J. Am. Chem. Soc.* **2003**, *125*, 4964−4965. (b) Capacchione, C.; D'Acunzi, M.; Motta, O.; Oliva, L.; Proto, A.; Okuda, J. *Macromol. Chem. Phys.* **2004**, *205*, 370−373. (c) Capacchione, C.; Proto, A.; Ebeling, H.; Mülhaupt, R.; Manivannan, R.; Möller, K.; Spaniol, T. P.; Okuda, J. *J. Mol. Catal. A: Chem.* **2004**, *213*, 137−140. (d) Beckerle, K.; Capacchione, C.; Ebeling, H.; Manivannan, R.; Mülhaupt, R.; Proto, A.; Spaniol, T. P.; Okuda, J. *J. Organomet. Chem.* **2004**, *689*, 4636−4641. (e) De Carlo, F.; Capacchione, C.; Schiavo, V.; Proto, A. *J. Polym. Sci., Part A: Polym. Chem.* **2006**, *44*, 1486−1491.

(12) Capacchione, C.; Manivannan, R.; Barone, M.; Beckerle, K.; Centore, R.; Oliva, L.; Proto, A.; Tuzi, A.; Spaniol, T. P.; Okuda, J. *Organometallics* **2005**, *24*, 2971−2982.

(13) Cohen, A.; Yeori, A.; Goldberg, I.; Kol, M. *Inorg. Chem.* **2007**, *46*, 8114−8116.

(14) (a) Atkinson, R. C. J.; Gerry, K.; Gibson, V. C.; Long, N. J.; Marshall, E. L.; West, L. J. *Organometallics* **2007**, *26*, 316−320. (b) Gregson, C. K. A.; Blackmore, I. J.; Gibson, V. C.; Long, N. J.; Marshall, E. L.; White, A. J. P. *Dalton Trans.* **2006**, 3134−3140. (c) Whitelaw, E. L.; Jones, M. D.; Mahon, M. F. *Inorg. Chem.* **2010**, *49*, 7176−7181.

(15) (a) El-Zoghbi, I.; Whitehorne, T. J. J.; Schaper, F. *Dalton Trans.* **2013**, *42*, 9376−9387. (b) Whitelaw, E. L.; Davidson, M. G.; Jones, M. D. *Chem. Commun.* **2011**, *47*, 10004−10006. (c) Romain, C.; Heinrich, B.; Laponnaz, S. B.; Dagorne, S. *Chem. Commun.* **2012**, *48*, 2213−2215. (d) Schwarz, A. D.; Thompson, A. L.; Mountford, P. *Inorg. Chem.* **2009**, *48*, 10442−10454.

(16) Darensbourg, D. J.; Karroonnirun, O. *Inorg. Chem.* **2010**, *49*, 2360−2371.

(17) (a) von Schenck, H.; Ryner, M.; Albertsson, A.; Svensson, M. *Macromolecules* **2002**, *35*, 1556−1562. (b) Marshall, E. L.; Gibson, V. C.; Rzepa, H. S. *J. Am. Chem. Soc.* **2005**, *127*, 6048−6051. (c) Barros, N.; Mountford, P.; Guillaume, S. M.; Maron, L. *Chem.—Eur. J.* **2008**, *14*, 5507−5518. (d) Dyer, H. E.; Huijser, S.; Susperregui, N.; Bonnet, F.; Schwarz, A. D.; Duchateau, R.; Maron, L.; Mountford, P. *Organometallics* **2010**, *29*, 3602−3621. (e) Börner, J.; dos Santos Vieira, I.; Pawlis, A.; Döring, A.; Kuckling, D.; Herres-Pawlis, S. *Chem.—Eur. J.* **2011**, *17*, 4507−4512. (f) d. S. Vieira, I.; Whitelaw, E. L.; Jones, M. D.; Herres-Pawlis, S. *Chem.—Eur. J.* **2013**, *19*, 4712−4716.

(18) Ajella, N.; Carpentier, J.-F.; Guillaume, C.; Helou, M.; Poirier, V.; Sarazin, Y.; Trifonov, A. *Dalton Trans.* **2010**, *39*, 8363−8376.

(19) (a) Ikpo, N.; Barbon, S. M.; Drover, M. W.; Dawe, L. N.; Kerton, F. M. *Organometallics* **2012**, *31*, 8145−8158. (b) Duda, A. *Macromolecules* **1994**, *27*, 576−582. (c) Duda, A. *Macromolecules* **1996**, *29*, 1399−1406. (d) Ning, Y.; Zhang, Y.; Rodriguez-Delgado, A.; Chen, E. Y.-X. *Organometallics* **2008**, *27*, 5632−5640.

(20) (a) Zhang, W.; Wang, Y.; Cao, J.; Wang, L.; Pan, Y.; Redshaw, C.; Sun, W.-H. *Organometallics* **2011**, *30*, 6253−6261. (b) Peng, K.-F.; Chen, C.-T. *Dalton Trans.* **2009**, 9800−9806. (c) Gamer, M. T.; Roesky, P. W.; Palard, I.; Le Hellaye, M.; Guillaume, S. M. *Organometallics* **2007**, *26*, 651−657.

(21) Vaartstra, B. A.; Huffman, J. C.; Gradeff, P. S.; Hubert-Pfalzgraf, L. G.; Daran, J.-C.; Parraud, S.; Yunlu, K.; Caulton, K. G. *Inorg. Chem.* **1990**, *29*, 3126−3131.

(22) Webster, R. L.; Noroozi, N.; Hatzikiriakos, S. G.; Thomson, J. A.; Schafer, L. L. *Chem. Commun.* **2013**, *49*, 57−59.

(23) (a) Thakur, K. A. M.; Kean, R. T.; Zell, M. T.; Padden, B. E.; Munson, E. J. *Chem. Commun.* **1998**, 1913−1914. (b) Thakur, K. A. M.; Kean, R. T.; Hall, E. S.; Kolstad, J. J.; Lindgren, T. A.; Doscotch, M. A.; Siepmann, J. I.; Munson, E. J. *Macromolecules* **1997**, *30*, 2422−2428.

(24) (a) Duda, A.; Kowalski, A.; Penczek, S. *Macromolecules* **1998**, *31*, 2114−2122. (b) Biela, T.; Duda, A.; Penczek, S. *Macromol. Symp.* **2002**, *183*, 1−10.

(25) Dines, J. *Heterocycl. Chem.* **1969**, *6*, 627−630.

(26) Frisch, M. J.; Trucks, G. W.; Schlegel, H. B.; Scuseria, G. E.; Robb, M. A.; Cheeseman, J. R.; Scalmani, G.; Barone, V.; Mennucci, B.; Petersson, G. A.; Nakatsuji, H.; Caricato, M.; Li, X.; Hratchian, H. P.; Izmaylov, A. F.; Bloino, J.; Zheng, G.; Sonnenberg, J. L.; Hada, M.; Ehara, M.; Toyota, K.; Fukuda, R.; Hasegawa, J.; Ishida, M.; Nakajima, T.; Honda, Y.; Kitao, O.; Nakai, H.; Vreven, T.; Montgomery, J. A., Jr.; Peralta, J. E.; Ogliaro, F.; Bearpark, M.; Heyd, J. J.; Brothers, E.; Kudin, K. N.; Staroverov, V. N.; Kobayashi, R.; Normand, J.; Raghavachari, K.; Rendell, A.; Burant, J. C.; Iyengar, S. S.; Tomasi, J.; Cossi, M.; Rega, N.; Millam, J. M.; Klene, M.; Knox, J. E.; Cross, J. B.; Bakken, V.; Adamo, C.; Jaramillo, J.; Gomperts, R.; Stratmann, R. E.; Yazyev, O.; Austin, A. J.; Cammi, R.; Pomelli, C.; Ochterski, J. W.; Martin, R. L.; Morokuma, K.; Zakrzewski, V. G.; Voth, G. A.; Salvador, P.; Dannenberg, J. J.; Dapprich, S.; Daniels, A. D.; Farkas, O.; Foresman, J. B.; Ortiz, J. V.; Cioslowski, J.; Fox, D. J. *Gaussian 09, revision A.02*; Gaussian, Inc.: Wallingford, CT, 2009.

(27) (a) Becke, A. D. *Phys. Rev. A* **1988**, *38*, 3098−3100. (b) Perdew, J. P. *Phys. Rev. B* **1986**, *33*, 8822−8824. (c) Perdew, J. P. *Phys. Rev. B* **1986**, *34*, 7406−7406.

(28) Hay, P. J.; Wadt, W. R. *J. Chem. Phys.* **1985**, *82*, 270−283.

(29) Schaefer, A.; Horn, H.; Ahlrichs, L. *J. Chem. Phys.* **1992**, *97*, 2571−2577.

(30) Chamberlain, B. M.; Cheng, M.; Moore, D. R.; Ovitt, T. M.; Lobkovsky, E. B.; Coates, G. W. *J. Am. Chem. Soc.* **2001**, *123*, 3229−3238.
(31) Legault, C. Y. CYLview, v1.0b, Université de Sherbrooke, 2009; http://www.cylview.org.
(32) Sheldrick, G. M. SADABS, Program for empirical absorption correction, University of Göttingen, Germany, 1996.
(33) Altomare, A.; Burla, M. C.; Camalli, M.; Cascarano, G. L.; Giacovazzo, C.; Guagliardi, A.; Moliterni, A. G. G.; Polidori, G.; Spagna, R. *J. Appl. Crystallogr.* **1999**, *32*, 115−119.
(34) Sheldrick, G. M. SHELX-97, University of Göttingen, Germany, 1997.
(35) ORTEP-3: Farrugia, L. J. *J. Appl. Crystallogr.* **1997**, *30*, 565−566.